Check for updates

Kinetics of the photolysis of pyridaben and its main photoproduct in aqueous environments under simulated solar irradiation†

Mengyuan Pan, Shiyin Mu, Yunfang Li, Ya Yang, Yuping Zhang, [ID] Lingzhu Chen [ID] * and Deyu Hu*

The photolytic fate of pyridaben and its main photolysis product was investigated in different aqueous solutions. Results showed that the photolysis of pyridaben followed pseudo first-order kinetics or the hockey-stick model. In buffer solutions, the half-life of pyridaben was the shortest at pH 4, while the degradation rate within 24 h was the highest at pH 9. Humic acids (HA) at concentrations of 1–20 mg L^{-1} favored the photolysis of pyridaben while fulvic acids (FA) did not have a significant effect. Nitrate at low concentrations (0.01 mM) accelerated the photolysis and Fe(III) at high concentrations (0.01 and 0.1 mM) significantly inhibited the photolysis. The photolysis rate of pyridaben in rainwater, tap water, and river water was significantly higher than that in distilled water. The half-lives in distilled water, rainwater, tap water, river water, and pond water were 2.36, 1.36, 1.61, 1.77, and 2.68 h, respectively. Ultra-high-performance liquid chromatography/high-resolution mass spectrometry identified M328 as a photolysis product. The degradation of M328 followed pseudo first-order kinetics in distilled water, buffer solutions and aqueous solutions fortified with HA. The half-lives of M328 were in the range of 7.07–13.95 h. These results are essential for further environmental risk assessment of pyridaben.

1. Introduction

Pyridaben (IUPAC name: 2-*tert*-butyl-5-(4-*tert*-butylbenzylthio)-4-chloropyridazin-3(2*H*)-one) (Fig. S1†) is a pyridazinone broad-spectrum acaricide developed by Nissan Chemical Industries Ltd in 1985.[1] Because of its low application dosage and quick effect, pyridaben has become the most widely used acaricide on citrus trees, apple trees, and cabbage to control pests (*e.g.*, red spider and yellow striped beetle).[1–4] It acts mainly by inhibiting the synthesis of glutamate dehydrogenase in the chromosomes of the muscle tissue, nerve tissue, and electron transport systems.[5,6] Pyridaben is the main ingredient of many commercial pesticide products on the agrochemical market. To date, 399 insecticide products containing pyridaben as the main ingredient have been registered in the China Pesticide Information Network (**https://www.chinapesticide.org.cn/hysj/index.jhtml**). After application, pesticides can enter natural waters *via* deposition and disperse with rainfall, surface runoff, and groundwater, consequently generating emerging pollutants in aquatic ecosystems.[7,8] The penetration of

pyridaben into ground water and surface water is limited due to its low solubility in water (0.22 mg L^{-1} at 20 °C).[2] Nevertheless, as an acaricide used worldwide, pyridaben has been detected in many rivers around the world at concentrations of up to 0.49 μg L^{-1},[9,10] which is higher than the permitted value of 0.1 μg L^{-1} specified for drinking water by the European Union (EU).[11] Ma *et al.* showed that pyridaben can cause severe cardiac malformations, functional abnormalities, and disrupts heart development gene expression in zebrafish.[1] Therefore, the fate of pyridaben in aqueous solutions must be understood to evaluate its potential hazard for aquatic ecosystems.

Photolysis is one of the most important abiotic conversion pathways for pesticides in the aqueous environment.[12,13] Photodegradation has significant effects on pesticide residues, efficacy, toxicity, and environmental safety.[8,14] The photolysis of organic pollutants leads to changes in their chemical structures and produces photolysis products.[15–18] Studies by Xu *et al.* and Villaverde *et al.* showed that the photolysis products of sulfapyridine and clethodim are much more toxic than their parent compounds.[19,20] The photolysis of a pesticide in an aqueous environment depends on its properties and the physicochemical characteristics of natural waterbodies.[21–23] In addition, the photolysis of a pesticide depends on its interactions with natural soluble substances such as humic acids (HA), fulvic acids (FA), nitrates, and Fe(III) ions.[19,24] Therefore, it is essential to understand the photolytic fate of a pesticide in the aqueous

State Key Laboratory Breeding Base of Green Pesticide and Agricultural Bioengineering, Key Laboratory of Green Pesticide and Agricultural Bioengineering, Ministry of Education, Guizhou University, Guiyang, P. R. China. E-mail: lzchen@gzu.edu.cn; gzu_dyhu@126.com; Fax: +86 88292090; Tel: +86 851 88292090

environment to evaluate the effects of its application and develop guidelines for its rational use.

At present, knowledge on the photolysis of pyridaben is limited. Zhu *et al.* studied the kinetics of photolysis of pyridaben in TiO_2 suspensions and surfactant cetyltrimethylammonium bromide aqueous dispersions using ultraviolet lamp irradiation, and photolysis products were qualitatively identified using gas chromatography-mass spectrometry (GC-MS).[24,25] However, the effects of various natural environmental factors, such as pH and soluble substances, on the photolysis of pyridaben and its products in aqueous environments have not been addressed. In addition, GC-MS has some drawbacks in the identification of transformation products. For instance, GC-MS is not suitable for the analysis of compounds that are difficult to volatilize, thermally unstable, or cannot be vaporized.[26] Many transformation products show a higher polarity than the parent compounds, which requires a derivatization step prior to GC-MS analysis.[27] Moreover, compounds that do not exist in the spectral library cannot be identified. In recent years, with the development and improvement of high-resolution mass spectrometry (HRMS) technology, ultra-high-performance liquid chromatography Q-Exactive Orbitrap HRMS (UPLC-HRMS) has been extensively applied for the qualitative and quantitative analyses of pesticides and their transformation products because of its high resolution, sensitivity, and accuracy.[7,28,29] In summary, it is necessary to investigate the effects of environmental factors on the photolysis of pyridaben and its products in aqueous environments using UPLC-HRMS.

This study aimed to comprehensively investigate the kinetics of the photolysis of pyridaben and its photolysis products in aqueous solutions using UPLC-HRMS under simulated solar irradiation. As the emission spectra of a xenon lamp is similar to that of sunlight, it was used as the light source.[22] UPLC-HRMS was employed for the qualitative and quantitative analyses of pyridaben and its photolysis products. The effects of pH, HA, FA, nitrates, and Fe(III) on the kinetics of photolysis pyridaben and its photolysis products were investigated. Finally, the photolysis of pyridaben was investigated in environmental waters. This research is essential for understanding the fate of pyridaben in aqueous environments and to provide guidance for its rational application.

2. Experimental

2.1 Materials and reagents

Pyridaben standards (99.8% purity) were provided by Dr Ehrenstorfer GmbH (Augsburg, Germany). The methanol used in UPLC-HRMS was supplied by Thermo Fisher Scientific Ltd (San Jose, CA, USA). HA was purchased from Hefei BASF Biotechnology Co. Ltd (Anhui, China). Analytical-grade sodium hydroxide was obtained from Chongqing Chuandong Chemical Co., Ltd (Chongqing, China). Potassium hydrogen phthalate was supplied by Tianjin Youpu Chemical Reagent Co. Ltd (Tianjin, China). Potassium dihydrogen phosphate and sodium nitrate were purchased from Chongqing Jiyuan Chemical Co. Ltd (Chongqing, China). Potassium chloride and

dichloromethane were provided by Tianjin Komiou Chemical Reagent Co. Ltd (Tianjin, China). Analytical grade boric acid was acquired from Chengdu Jinshan Chemical Reagent Co., Ltd (Chengdu, China). Ferric chloride hexahydrate, anhydrous sodium sulfate, and sodium chloride were obtained from Tianjin Zhiyuan Chemical Reagent Co. Ltd (Tianjin, China). Distilled water was supplied by Watsons Co. Ltd (Dongguan, China). The physicochemical characteristics of distilled water is listed in Table S1.†

A stock solution of pyridaben was prepared using methanol, with a concentration of 2500 mg L^{-1}. A series of working standard solutions of pyridaben, with concentrations of 2, 1, 0.2, 0.1, 0.02, and 0.01 mg L^{-1}, were prepared by serial dilution with methanol. The standard solutions were stored at 4 °C in the dark.

2.2 Tap water and natural water sampling

Tap water samples were collected from the Fine Chemical Research and Development Center of Guizhou University. Rainwater samples were collected from an open space at Guizhou University on September 13, 2021. River and pond water samples were collected from the Huaxi River (Guiyang, Guizhou Province) and a pond near a citrus garden in the Guizhou University teaching experimental field, respectively. All water samples were used without pretreatment. The pH and dissolved organic carbon of the water samples were measured using a pH meter (PB-10, Sartorius Scientific Instruments Co., Ltd, Beijing, China) and fully automatic total organic carbon analyzer (Vario TOC, DKSH Commercial Co., Ltd, Shanghai, China). The conductivity, salinity, and total dissolved solids were measured using a portable conductivity meter (DDBJ-350, Shanghai INESA Scientific Instrument Co., Ltd, Shanghai, China). The physicochemical characteristics of the water samples are listed in Table S1.†

2.3 Photolysis procedure

Photolysis was performed using a photochemical apparatus (BL-GHX-V, Shanghai Bilon Instrument Co., Ltd, Shanghai, China) equipped with a 500 W xenon lamp ($\lambda \geq 290$ nm) and a quartz cold trap. Samples were magnetically stirred and irradiated in a quartz tube 8 cm from the lamp. Each quartz tube contained 30 mL of aqueous solution. The photolysis experiments were conducted in triplicate at a temperature of 20 ± 1 °C. At various time intervals (0, 1, 3, 5, 7, 10, 12, 24, 30, 36 and 48 h), aliquots of 1 mL were removed from every quartz tube, filtered using a 0.22 μm nylon membrane and injected into the UPLC-HRMS intermediately for qualitative and quantitative analyses.

Photolysis experiments were performed at an initial concentration of 2.0 mg L^{-1} of pyridaben. MeOH was used as a cosolvent to facilitate the dissolution of pyridaben in water. The photolysis samples were prepared by adding 0.08 mL of the pyridaben stock solutions (2500 mg L^{-1} in MeOH) into 100 mL of buffer solutions and distilled water. The effect of pH was investigated using buffer solutions with pH values of 4, 7, and 9. All buffer solutions (pH 4, 7, and 9) were prepared with distilled water obtained from Watsons Co., Ltd, as previously described.[22] Buffer solutions and

glass apparatuses were sterilized by autoclaving for 40 min at 120 °C to avoid microbial degradation. The pH of each solution was measured and calibrated prior to the experiments. The effects of different natural substances at different levels: HA at 1, 5, 10, and 20 mg L^{-1}; FA at 1, 10, and 20 mg L^{-1}; nitrates at 0.01, 0.1, and 1 mM; and Fe(III) at 0.001, 0.01, and 0.1 mM were investigated in distilled water solutions. The photolysis of pyridaben in different water matrices were investigated in water samples collected in Section 2.2.

2.4 Analytical procedure

UPLC-HRMS analysis was performed on an Ultimate 3000 RS (Dionex, Sunnyvale, CA, USA) coupled with a Q-Exactive Orbitrap mass spectrometer (Thermo Fischer Scientific, MA, USA). Samples were detected with a heated electrospray interface in positive ionization mode. Chromatographic separation was performed on a reversed-phase InertSustainSwift C$_{18}$ column (2.1 × 100 mm i.d., 1.9 μm) (GL Sciences, Tokyo, Japan), and the temperature of the column was set to 40 °C. Chromatographic analysis was performed using gradient elution with a mobile phase consisting of distilled water (A) and methanol (B). The mobile phase gradient was: 0 min, B 60%; 0.5 min, B 60%; 5 min, B 95%; 9 min, B 95%; 9.5 min, B 60%; 15 min, B. 60%. The flow rate was 0.2 mL min^{-1}, and the photolysis sample injection volume was 2 μL. Qualitative and quantitative analyses of the aqueous samples were performed in the full-scan/data-dependent acquisition (full-MS/ddMS^2) mode. The optimized mass spectra parameters were as follows: auxiliary gas heater temperature, 300 °C; capillary temperature, 350 °C; spray voltage, 2.5 kV, flow rates of sheath, sweep, and auxiliary gases at 35, 0, and 10 a.u., respectively. All MS^2 data were acquired using the following conditions: AGC target, 1.0 × 10^5; maximum injection time, 50 ms; isolation window, 2 m/z; microscan, 1. The resolution was set at 17 500. Collision energies were gradually set to 10, 30, and 50. Pyridaben and M328 were analyzed by their quasi-molecular ions with exact ion mass of 365.14489 and 329.16821, respectively.

2.5 Data processing

The photolysis of pyridaben followed the pseudo first-order kinetics or the hockey-stick model. Pseudo first-order kinetics was described using eqn (1):

$$C_t = C_0\,e^{-kt} \tag{1}$$

where C_t is the concentration of pyridaben residue at time t (mg L^{-1}), C_0 is the initial concentration (mg L^{-1}), t is the irradiation time (h), and k is the degradation rate constant (h^{-1}). The half-life value ($t_{1/2}$) was estimated using eqn (2):

$$t_{1/2} = \frac{\ln 2}{k} \tag{2}$$

Hockey-stick model was described using eqn (3) and (4):

$$C_t = C_0\,e^{-k_1 t}\,(t \le t_{\mathrm{b}}) \tag{3}$$

$$C_{\mathrm{t}} = C_0\,e^{-k_1 t_{\mathrm{b}}}\,e^{-k_2(t-t_{\mathrm{b}})}\,(t > t_{\mathrm{b}}) \tag{4}$$

where C_{t} is the concentration of pyridaben at time t (mg L^{-1}), C_0 is the initial concentration (mg L^{-1}), k_1 is the rate constant before the break point (h^{-1}), k_2 is the rate constant after the break point (h^{-1}) and t_{b} is the break point (h). The half-life value ($t_{1/2}$) was estimated using eqn (5) and (6):

$$t_{1/2} = \frac{\ln 2}{k_1}\,\bigl(t_{1/2} \le t_{\mathrm{b}}\bigr) \tag{5}$$

$$t_{1/2} = t_{\mathrm{b}} + \frac{\ln 2 - k_1 t_{\mathrm{b}}}{k_2}\,\bigl(t_{1/2} > t_{\mathrm{b}}\bigr) \tag{6}$$

The concentration–time relationship of M328 in the degradation phase of evolution curves was fitted. The fit was started after the inflection points of the evolution curve, and at least six points were used. The degradation of M328 in the buffer solutions, distilled water and distilled water fortified with HA followed a pseudo first-order reaction (eqn (1)), and $t_{1/2}$ was calculated with eqn (2).

All statistical analyses were accomplished using IBM SPSS Statistics 24.0 software (SPSS Inc., Chicago, IL, USA). All half-life values were described as mean ± standard deviation (SD) of triplicate data. The differences between treatments and control were compared at a confidence level of 0.05 with one-way analysis of variance (ANOVA).

3. Results and discussion

3.1 Validation of analytical method

The performance of the analytical method for pyridaben detection was evaluated. Pyridaben showed a symmetrical peak shape with a retention time of 8.46 min (Fig. S2a†). The standard curve of pyridaben was plotted using the peak area as the ordinate and concentration as the abscissa. The linear regression equation of pyridaben was $y = 6\,478\,090x + 74\,716$, with a coefficient of determination (R^2) of 0.9996 at a concentration range of 0.01–2.00 mg L^{-1}. These results demonstrate that the analytical method performed well.

3.2 Identification of photolysis product

Post-collection data mining was carried out using Compound Discoverer 2.0 software to screen for the photolysis products of pyridaben. Monoisotopic peaks of ^{35}Cl and ^{37}Cl were observed for the parent compound with mass-to-charge ratios (m/z) of 365.14362 and 367.14035, respectively (Fig. S3a†). In addition, MS^2 fragments, which provide structural diagnostic information, are shown in Fig. S3b.† The main fragment ions had an m/z of 309.08115, which resulted from the loss of (CH$_3$)$_3$C, and an m/z of 147.11650 corresponding to [(CH$_3$)$_3$CC$_6$H$_4$CH$_2$]$^+$. The extracted ion chromatogram of the 12 h photolysis sample in distilled water is shown in Fig. S2b.† In addition to the parent compound, one more peak was detected at 8.71 min (Fig. S2b†), presenting an m/z of 328.16039 (Fig. S4a†) with the molecular formula C$_{19}$H$_{24}$N$_2$OS (M328). M328 was identified as 2,9-di-*tert*-butyl-2,6-dihydro-1*H*-isothiochromeno[3,4-*d*]pyridazin-1-one,

as reported by EFSA.[2] The formation of M328 can be attributed to the intramolecular elimination of HCl from pyridaben, resulting in the formation of a cyclization product. The structure of M328 was verified using reasonable structures of fragment ions illustrated in Fig. S4b.† The main fragment ions had an m/z of 273.10492, resulting from the loss of $(CH_3)_3C$, and an $m/z = 217.04259$, resulting from the loss of another $(CH_3)_3C$ and subsequent rearrangement. Mass spectral data for pyridaben and M328 are summarized in Table 1.

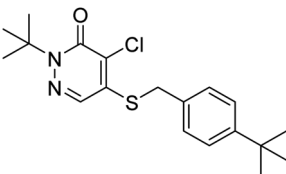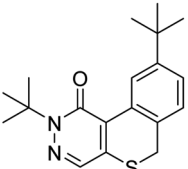### 3.3 Kinetics of photolysis of pyridaben and M328

Dark control experiments using distilled water and buffer solutions of pH 4, 7, and 9 were carried out for 24 h to investigate the hydrolysis rate of pyridaben. Results showed that pyridaben did not significantly decrease within 24 h, with a degradation rate of less than 13% (Fig. S5†). Thus, during irradiation over 24 h, the hydrolysis of pyridaben was negligible, and the degradation of pyridaben in aqueous solutions was mainly governed by photolysis. The kinetic parameters of the photolysis of pyridaben and M328 under different conditions are summarized in Tables S2 and S3.†

3.3.1 Effects of pH. Previous studies have shown that the fate of photolysis products and the dissociation of pesticides in natural waters are affected by pH.[12,23] Therefore, the effect of pH on the photolysis of pyridaben was investigated. After 24 h of xenon lamp irradiation, the degradation rates of pyridaben in distilled water, and acidic, neutral, and alkaline buffer solutions were 93.50%, 93.00%, 96.24%, and 99.50%, respectively. As shown in Fig. 1a, the photolysis of pyridaben in neutral and alkaline buffer solutions can be well described using pseudo first-order reaction kinetics, while the photolysis in acidic buffer solution and distilled water followed the hockey-stick model. The half-lives were 2.36, 1.91, 5.46, and 3.47 h in distilled water and pH 4, 7, and 9 buffer solutions, respectively (Table S2†). A

significance analysis revealed that the photolysis of pyridaben was pH dependent ($p < 0.05$, Fig. 2). Under acidic conditions, the half-life of pyridaben was the shortest. The same results were observed for the photolysis of nitrofurantoin,[30] hexaflumuron,[31] and metribuzin.[32] Fig. 3a shows that M328 attained its maximum quantity after the irradiation of pyridaben in distilled water for approximately 3 h, and it then gradually decreased with increasing irradiation time. In the buffer solutions of pH 4, 7, and 9, the quantity of M328 peaked 10 h after irradiation and then gradually degraded. The degradation phase of the evolution curves followed the pseudo first-order kinetic model (Fig. S6†). Compared with neutral and alkaline conditions, acidic conditions promoted the formation of M328 (Fig. 3a), while inhibited the degradation of M328 ($p < 0.05$, Fig. 4). The degradation half-lives of M328 were 9.37, 13.95, 12.16, and 11.46 h in distilled water, acidic, neutral and alkaline buffer solutions, respectively (Table S3†), which were longer than those of pyridaben (Table S2†).

3.3.2 Effects of HA. HA is a predominant constituent of dissolved organic matter that is widely present in surface waters.[12,33] Studies have demonstrated that HA has a complex effect on the photolysis of organic compounds in natural waters.[33,34] Therefore, the effects of HA on the photolysis of pyridaben were investigated. The kinetics of pyridaben with different concentrations of HA agreed with the hockey-stick model (Fig. 1b). In general, HA favors the photolysis of pyridaben in an aqueous solution. The half-lives of pyridaben were 1.47, 1.44, 1.62, and 1.94 h in aqueous solutions fortified with HA concentrations of 1, 5, 10, and 20 mg L^{-1}, respectively (Table S2†). The photolysis rate of pyridaben was related to the concentration of HA, and the promoting effect of HA was more significant at low concentrations ($p < 0.05$, Fig. 2). The presence of HA can promote the photolysis by accelerating the energy transfer and electron transfer to the ground state of organic

Table 1 Mass spectra and structural data of pyridaben and M328

| Compound | t_R (min) | Ions | | Error (ppm) | Elemental composition |
		Measured mass	Theoretical mass		
Pyridaben	8.46	365.14362	365.14489	−3.49	$C_{19}H_{26}ON_2ClS$ ([M + H]$^+$)
		309.08115	309.08229	−3.69	$C_{15}H_{18}ON_2ClS$
		147.11650	147.11683	−2.22	$C_{11}H_{15}$
		132.09305	132.09335	−2.27	$C_{10}H_{12}$
		119.08549	119.08553	−0.33	C_9H_{11}
		105.07007	105.06988	1.81	C_8H_9
M328	8.71	329.16742	329.16821	−2.40	$C_{19}H_{25}ON_2S$ ([M + H]$^+$)
		273.10492	273.10561	−2.53	$C_{15}H_{17}ON_2S$
		258.08130	258.08214	−3.24	$C_{14}H_{14}ON_2S$
		217.04259	217.04301	−1.95	$C_{11}H_9ON_2S$
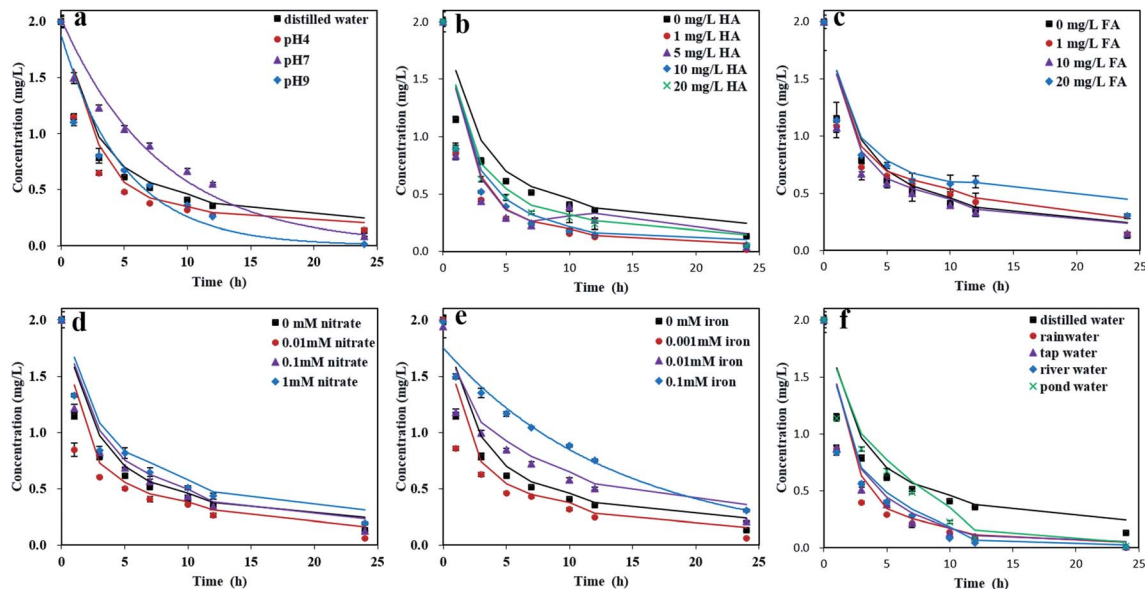
Fig. 1   The photolysis kinetics of pyridaben in buffer solutions (pH = 4.00, 7.00, and 9.00) and distilled water (pH = 5.50) (a) and distilled waters fortified with HA (b), FA (c), nitrate (d), iron (e), and tap water and natural waters (f).
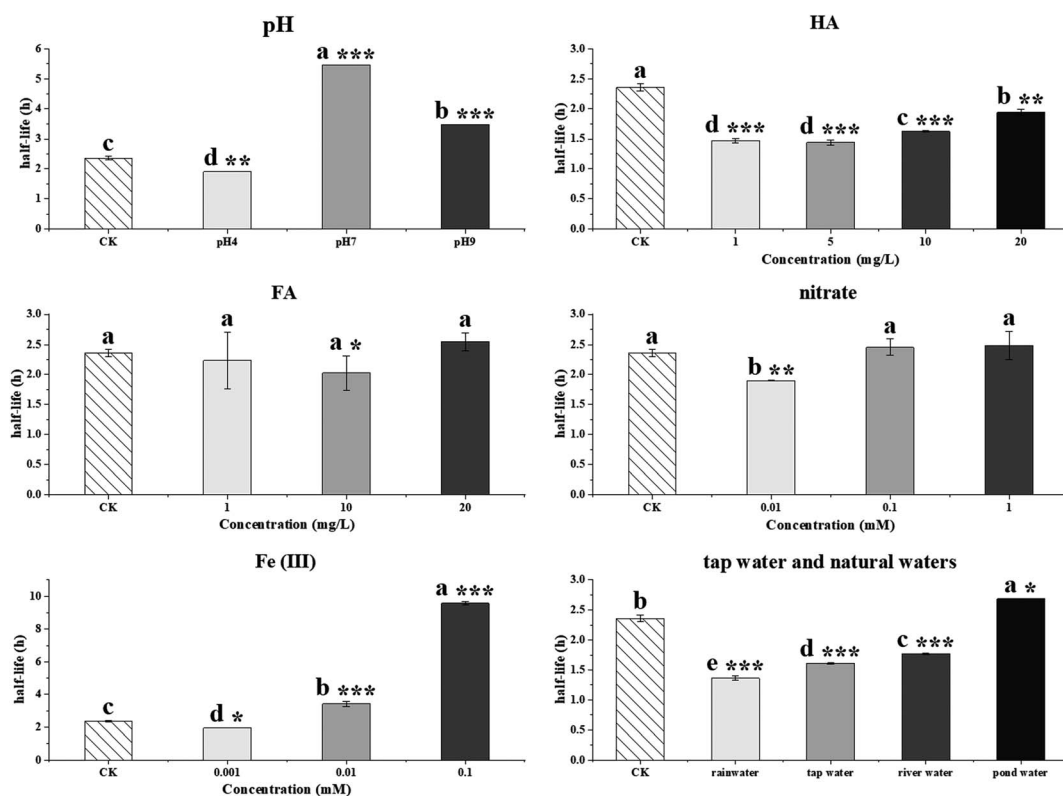

Fig. 2   The half-lives of photolysis for pyridaben in the different aqueous solutions. (Letters on the bars indicate significance levels between treatments and control based on $p < 0.05$. Asterisks on the bars indicate significance levels between treatments and control: * indicate $p < 0.05$, ** indicate $p < 0.01$, *** indicate $p < 0.001$).

compounds (*e.g.*, from the excited HA state), and generating reactive species (*e.g.*, singlet oxygen, hydroxyl radicals, and [3]HA*) as well.[17,35] The similar results were also observed for the photolysis of tetracycline,[16] hexaflumuron,[31] and 17β-

Estradiol.[36] The evolution curve of M328 in HA solutions is shown in Fig. 3b. The quantity of M328 increased rapidly with the degradation of pyridaben and then gradually decreased after reaching a maximum value. With an increase in HA, the
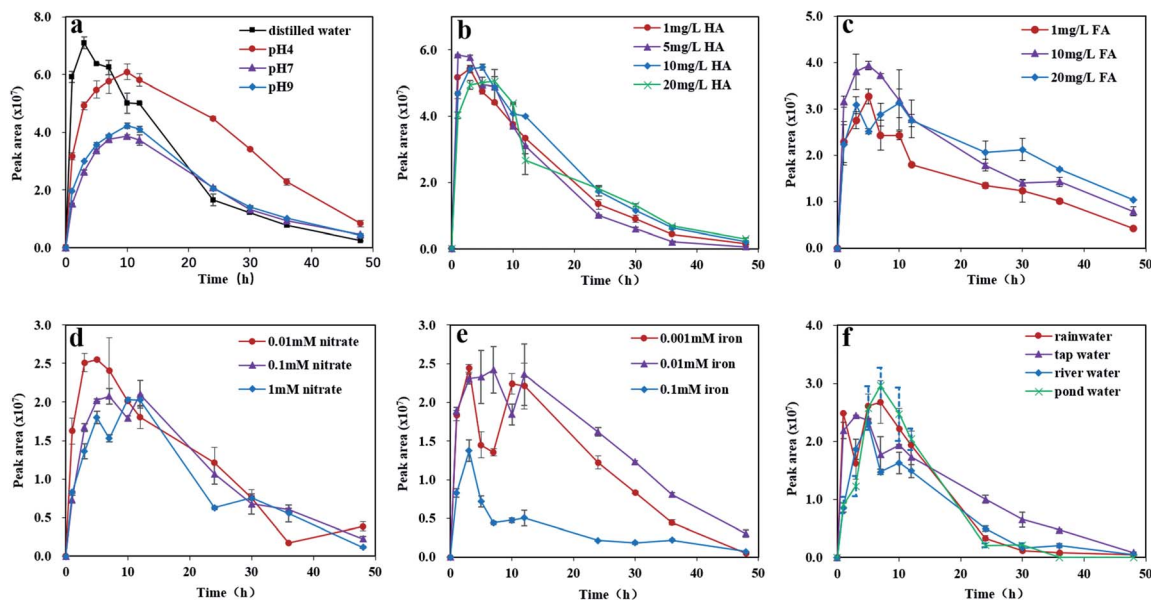
Fig. 3 The evolution of M328 in buffer solutions (pH = 4.00, 7.00, and 9.00) and distilled waters (pH = 5.50) (a) and distilled waters fortified with HA (b), FA (c), nitrate (d), iron (e), and tap water and natural waters (f).
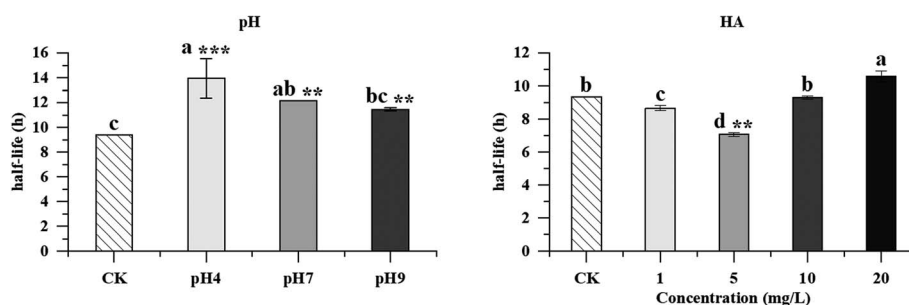

Fig. 4 The half-lives of degradation for M328 in distilled water, buffer solutions and HA solutions (Letters on the bars indicate significance levels between treatments and control based on $p < 0.05$. Asterisks on the bars indicate significance levels between treatments and control: ** indicate $p < 0.05$, ** indicate $p < 0.01$, *** indicate $p < 0.001$.).

inflection points shifted to the right, ranging from 1 to 7 h. The degradation trend of M328 fitted well with the first-order kinetics model (Fig. S7†). The half-lives of M328 in HA solutions with concentrations of 1, 5, 10, and 20 mg L^{-1} were 8.67, 7.07, 9.30, and 10.59 h, respectively (Table S3†). The degradation of M328 in HA solutions was dose dependent ($p < 0.05$, Fig. 4).

3.3.3 Effects of FA. FA is another predominant constituent of dissolved organic matter.[23] The role of FA in pyridaben photolysis was investigated at concentrations of 1, 10, and 20 mg L^{-1}. The kinetics of pyridaben with different concentrations of FA agreed with the hockey-stick model (Fig. 1c), with half-lives ranging from 2.02 to 2.54 h (Table S2†). The results of significance analysis suggested that the photolysis rate of pyridaben was unrelated to the concentration of FA ($p > 0.05$, Fig. 2). The evolution curve of M328 in FA solution is shown in Fig. 3c. The quantity of M328 increased rapidly with the degradation of pyridaben, and then gradually decreased, with the inflection point occurring at between 5 and 10 h of irradiation.

3.3.4 Effects of nitrates. The effects of nitrate on the photolysis of pyridaben were investigated at concentrations of 0.01, 0.1, and 1 mM based on the levels detected in natural waters.[12,18] The kinetics of the photolysis of pyridaben with different concentrations of nitrates agreed with the hockey-stick model (Fig. 1d), and the half-lives were in the range of 1.90–2.48 h (Table S2†). Compared with photolysis in distilled water, the photolysis of pyridaben was promoted with nitrate at low concentrations (0.01 mM) ($p < 0.01$, Fig. 2 and Table S2†). However, nitrate at concentration of 0.1 mM and 1 mM had a slight effect on the photolysis of pyridaben ($p > 0.05$, Fig. 2 and Table S2†). Previous studies have demonstrated that nitrate exhibited conflicting effects on the photolysis of organic compounds. Xu *et al.* reported that nitrate at concentrations from 0.5 to 10 mM did not play an important role in the photolysis of sulfapyridine.[18] However, Dong *et al.* observed that nitrates at 5 and 10 mg L^{-1} marginally accelerated the photolysis of fluopyram and then inhibited it with a further increase in concentration.[23] On the one hand, nitrates are a major source of

hydroxyl radicals, which was beneficial to the photolysis of organic compounds.[31,35,37,38] On the other hand, nitrate had a scavenging effect on hydroxyl radicals at high concentrations, which inhibited the photolysis of organic compounds.[23,35,38] The UV-vis spectra of nitrates showed that the absorbance of nitrates increased with increasing concentration at $\lambda \geq 290$ nm (Fig. S8c†); thus, the inhibitory effects of nitrates increased with an increasing concentration. The evolution curves of M328 indicated that nitrates at low concentrations promoted the formation of M328 (Fig. 3d). The quantity of M328 in aqueous solutions fortified with nitrates at concentrations of 0.01, 0.1, and 1 mM reached a maximum after irradiation for approximately 5, 12, and 10 h, respectively, and then gradually decreased as the irradiation time increased.

3.3.5 Effects of Fe(III).

Fe(III) is a representative component of natural waters with concentrations of 10^{-7} to 10^{-4} M, and it plays an important role in the photolysis of pesticides.[39] In this study, ferric chloride hexahydrate was used as the source of Fe(III) to study its effects on pyridaben photolysis. The photolysis of pyridaben at different concentrations of Fe(III) agreed with pseudo first-order kinetics or the hockey-stick model (Fig. 1e), with half-lives ranging from 1.95 to 9.56 h as the Fe(III) concentration increased from 0.001 to 0.1 mM (Table S2†). The photolysis of pyridaben was significantly inhibited at high Fe(III) concentration compared with photolysis in distilled water ($p <$ 0.001, Fig. 2 and Table S2†). Previous studies have demonstrated that the degradation of organic pollutants is dose dependent in the presence of Fe(III). For example, Lin *et al.* noticed that Fe(III) can marginally promote the photolysis of fluazaindolizine at a concentration of 0.1–5 mg L^{-1}.[12] Nevertheless, Li *et al.* observed that Fe(III) inhibited the photolysis of oxytetracycline at concentrations of 2.5–15 mM.[39] Fang *et al.* also reported that the photolysis of flupyradifurone was inhibited in the Fe(III) solutions, and the photolysis rate gradually slowed with increasing Fe(III) concentrations.[40] Fe(III) could generate ·OH *via* the following reactions:[41,42]

$$Fe^{3+} + H_2O \rightleftharpoons Fe(OH)^{2+} + H^+$$

$$Fe(OH)^{2+} + h\nu \rightarrow Fe^{2+} + \cdot OH$$
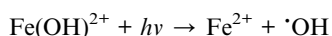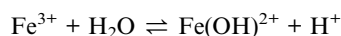
Under acidic conditions, the formation of Fe(OH)$^{2+}$ is inhibited, thereby inhibiting the formation of hydroxyl radical. The pH values of Fe(III) solutions with concentrations at 0.001, 0.01, and 0.1 mM were 5.73, 4.97, and 3.78, respectively. Therefore, the photolysis rate of pyridaben was slower in solutions with higher concentrations of Fe(III) due to the presence of more hydrogen ions and fewer hydroxyl radicals. In addition, overlaps between the absorptions of Fe(III) and pyridaben were observed at $\lambda \geq 290$ nm (Fig. S8d†). Thus, under xenon lamp irradiation, pyridaben and Fe(III) competed for photons, and this competition increased with the increasing of Fe(III) concentration. Overall, Fe(III) exhibited an inhibitory effect at high concentrations for the photolysis of pyridaben. The evolution curve of M328 in Fe(III) solutions is shown in Fig. 3e. The concentration of M328 reached a maximum after 3–7 h of

irradiation in the Fe(III) solutions at concentrations of 0.001–0.1 mM. However, in one Fe(III) solution (0.1 mM), the formation of M328 was significantly inhibited, which may have been caused by the low photolysis rate of pyridaben (Fig. 3e).

3.3.6 Photolysis in tap water and natural waters.

To obtain a better understanding of the comprehensive photolytic fate of pyridaben in aqueous environments, its photolysis kinetics were investigated in tap water, rainwater, river water, and pond water. The degradation of pyridaben under dark conditions was shown in Fig. S9.† Results showed that the 24 h degradation rates of pyridaben in rainwater, river water, pond water, and tap water were 16.50%, 5.50%, 1.00%, and 7.50%, respectively. The photolysis kinetics of pyridaben in the four water samples followed the hockey-stick model (Fig. 1f). The half-lives of pyridaben were 1.36, 1.61, 1.77, and 2.68 h in rainwater, tap water, river water, and pond water samples, respectively (Table S2†). Compared with photolysis in distilled water, the photolysis rate of pyridaben was significantly accelerated in tap water, rainwater and river water ($p < 0.001$, Fig. 2 and Table S2†), while was inhibited in pond water ($p < 0.05$, Fig. 2 and Table S2†). These results can be attributed to the combined effects of the compositions and pH of the water samples.[33] The photolysis rates of pyridaben in natural waters have a correlation with the levels of dissolved organic carbon (DOC) (Table S1†). In general, higher DOC level indicated slower photolysis rate. The short half-life of pyridaben in rainwater can be attributed to the high degradation rate under dark conditions and low pH value of rainwater. The formation and evolution of M328 in environmental waters are shown in Fig. 3f. The quantity of M328 reached its peak value after irradiation for 3–7 h and it then gradually decreased with increasing irradiation time.

4. Conclusions

In this paper, the photolysis behaviors of pyridaben and its main photolysis product in aqueous solutions were comprehensively investigated. The photolysis of pyridaben followed the pseudo first-order kinetics in neutral and alkaline buffer solutions, and 0.1 mM Fe(III) solution, while followed hockey-stick model in distilled water, acidic buffer solution, and aqueous solutions fortified with HA, FA, nitrate, and low concentration of Fe(III) (0.001 and 0.01 mM). The photolysis of pyridaben was pH dependent. The half-life of pyridaben in acidic buffer solution was shorter than that in neutral and alkaline buffer solutions. For dissolved organic matter, HA at concentrations of 1–20 mg L^{-1} favored the photolysis of pyridaben while FA had a slight effect on photolysis. For inorganic ions, nitrate at low concentrations accelerated the photolysis and Fe(III) at high concentrations significantly inhibited the photolysis. The photolysis of pyridaben in tap water and natural waters followed hockey-stick model, with half-lives of 1.36–2.68 h. Compound M328, resulting from cyclization *via* the loss of HCl, was identified as the photolysis product of pyridaben using UPLC-HRMS. In the photolysis process, the quantity of M328 first increased with the degradation of pyridaben, and then gradually degraded after reaching the peak value within 48 h. The degradation of M328 in distilled water, buffer solutions, and

aqueous solutions fortified with HA fitted well with pseudo first-order kinetics, with half-lives ranging from 7.07 to 13.95 h. These results are important for understanding the environmental behavior of pyridaben in aqueous environments and can guide its rational use. Further toxicity studies should be conducted on M328 and photolysis solutions to evaluate the risk to aquatic organisms during the photolysis of pyridaben.

Author contributions

M. Pan performed the experiment, analyzed the data, and wrote the manuscript. S. Mu, Y. Li and Y. Yang discussed the project. Y. Zhang helped perform the analysis with constructive discussions. L. Chen, and D. Hu supervised the whole project and directed the writing of the manuscript.

Conflicts of interest

There are no conflicts of interest to declare.

Acknowledgements

References

1 J. Ma, Y. Huang, P. Jiang, Z. Liu, Q. Luo, K. Zhong, W. Yuan, Y. Meng and H. Lu, *Aquat. Toxicol.*, 2021, **237**, 105870.
2 European Food Safety Authority (EFSA), *EFSA J.*, 2010, **8**, 1632.
3 N. Wang, S. Zhao, X. Long, J. Gong, C. Sui, Y. Zhang, L. Chen and D. Hu, *J. Environ. Sci. Health, Part B*, 2020, **55**, 613–619.
4 X. Zhu, X. Feng, C. Yuan, X. Cao and J. Li, *J. Mol. Catal. A: Chem.*, 2004, **214**, 293–300.
5 C. Gomez, M. J. Bandez and A. Navarro, *Front. Biosci.*, 2007, **12**, 1079.
6 J. Liu, X. Xu, A. Wu, Z. Wang, S. Song, H. Kuang, L. Liu and C. Xu, *Microchem. J.*, 2021, **170**, 106762.
7 L. R. Zeng, L. H. Shi, X. G. Meng, J. Xu, G. F. Jia, T. Gui, Y. P. Zhang and Y. Hu, *J. Environ. Sci. Health, Part B*, 2019, **54**, 317–325.
8 L. Lian, B. Jiang, Y. Xing and N. Zhang, *Ecotoxicol. Environ. Saf.*, 2021, **224**, 112655.
9 S. Zheng, B. Chen, X. Qiu, M. Chen, Z. Ma and X. Yu, *Chemosphere*, 2016, **144**, 1177–1192.
10 Y. Jabali, M. Millet and M. El-Hoz, *Environ. Sci. Pollut. Res.*, 2020, **27**, 17997–18012.
11 European Union (EU), *Community Trade Mark Regulation*, 2015, pp. 1478–1488.
12 H. Lin, K. Pang, Y. Ma and J. Hu, *Chemosphere*, 2019, **214**, 543–552.
13 C. K. Remucal, *Environ. Sci.: Processes Impacts*, 2014, **16**, 628.
14 C. C. Kaonga, K. Takeda and H. Sakugawa, *Chemosphere*, 2016, **145**, 256–264.
15 K. Chen, F. Tian, C. Wu, X. Wu, J. Xu, F. Dong, X. Liu and Y. Zheng, *Water Res.*, 2019, **161**, 531–539.
16 C. Ma, X. Liu, X. Wu, F. Dong, J. Xu and Y. Zheng, *J. Hazard. Mater.*, 2021, **403**, 124033.
17 S. Jiao, S. Zheng, D. Yin, L. Wang and L. Chen, *Chemosphere*, 2008, **73**, 377–382.
18 J. Xu, Z. Hao, C. Guo, Y. Zhang, Y. He and W. Meng, *Chemosphere*, 2014, **99**, 186–191.
19 J. J. Villaverde, B. Sevilla-Morán, C. López-Goti, L. Calvo, J. L. Alonso-Prados and P. Sandín-España, *Sci. Total Environ.*, 2018, **615**, 643–651.
20 B. Sevilla-Morán, L. Calvo, C. López-Goti, J. L. Alonso-Prados and P. Sandín-España, *Chemosphere*, 2017, **168**, 501–507.
21 V. Lavtižar, C. A. M. van Gestel, D. Dolenc and P. Trebše, *Chemosphere*, 2014, **95**, 408–414.
22 Y. Man, M. Stenrød, C. Wu, M. Almvik, R. Holten, J. L. Clarke, S. Yuan, X. Wu, J. Xu, F. Dong, Y. Zheng and X. Liu, *J. Hazard. Mater.*, 2021, **418**, 126303.
23 B. Dong and J. Hu, *Environ. Sci. Pollut. Res.*, 2016, **23**, 19096–19106.
24 X. Zhu, C. Yuan, Y. Bao, J. Yang and Y. Wu, *J. Mol. Catal. A: Chem.*, 2005, **229**, 95–105.
25 X. Zhu, C. Yuan and H. Chen, *Environ. Sci. Technol.*, 2007, **41**, 263–269.
26 A. Agüera, L. Estrada, I. Ferrer, E. M. Thurman, S. Malato and A. R. Fernández-Alba, *J. Mass Spectrom.*, 2010, **40**, 908–915.
27 J. L. Martínez Vidal, P. Plaza-Bolaños, R. Romero-González and A. Garrido Frenich, *J. Chromatogr. A*, 2009, **1216**, 6767–6788.
28 C. Jiang, H. Han, J. Dai, Z. Wang, Y. Chai, C. Wang, X. Liu, C. Lu and H. Chen, *Food Chem.*, 2022, **367**, 130662.
29 H. Chen, G. Gao, P. Liu, M. Pan, Y. Chai, X. Liu and C. Lu, *Food Chem.*, 2018, **246**, 328–334.
30 M. Biošić, D. Dabić, I. Škorić and S. Babić, *Environ. Sci.: Processes Impacts*, 2021, **23**, 1385–1393.
31 C. Lu, X. Yin, X. Liu and M. Wang, *Photochem. Photobiol.*, 2014, **90**, 1219–1223.
32 H. Liu and L. Guan, *Adv. Mat. Res.*, 2012, **518–523**, 436–439.
33 Y. Bao and J. Niu, *Chemosphere*, 2015, **134**, 550–556.
34 Y. Zhang, J. Li, L. Zhou, G. Wang, Y. Feng, Z. Wang and X. Yang, *Environ. Sci. Pollut. Res.*, 2016, **23**, 6982–6989.
35 Z. Zhang, X. Xie, Z. Yu and H. Cheng, *Water Res.*, 2019, **148**, 19–29.
36 Y. Liu, H. Sun, L. Zhang and L. Feng, *Process Saf. Environ.*, 2017, **112**, 335–341.
37 E. Koumaki, D. Mamais, C. Noutsopoulos, M. Nika, A. A. Bletsou, N. S. Thomaidis, A. Eftaxias and G. Stratogianni, *Chemosphere*, 2015, **138**, 675–681.
38 J. Niu, Y. Li and W. Wang, *Chemosphere*, 2013, **92**, 1423–1429.
39 C. Li, D. Zhang, J. Peng and X. Li, *J. Photochem. Photobiol., A*, 2018, **356**, 239–247.
40 N. Fang, Z. Lu, Z. Hou, C. Zhang and X. Zhao, *Chemosphere*, 2022, **298**, 134294.
41 Q. Zhao, H. Zhao, X. Quan, S. Chen and Y. Zhang, *Mar. Pollut. Bull.*, 2014, **86**, 76–83.
42 S. Sun, J. Jiang, H. Zhao, H. Wan and B. Qu, *Chemosphere*, 2020, **241**, 124971.